iJET EXPLORE International Journal of Engineering & Technology
CENTRE OF PROFESSIONAL RESEARCH PUBLICATIONS
ISSN 2049-3444

International Journal of Engineering and Technology Volume 2 No. 3, March, 2012

A Study on the Scale Effect on Bearing Capacity and Settlement of Shallow Foundations

Bestun J. Nareeman
Geotechnical Engineering Department, University of Koya, Koya-Erbil, Iraq

ABSTRACT

This paper investigates the effect of scale on the bearing capacity and settlement of footings. For this study, three types of prototype footing circular, square and rectangular were investigated . For the circular footing, diameters (8, 10, 15 and 20 cm) were used, while for the square and rectangular footings, the dimensions used were 8×8, 10×10, 15×15, 20×20 cm and 8×12, 10×15,15×22.5 and 20×30 cm, respectively. The experimental work was complimented by finite element studies using the software (SAGE-CRISP), which is a 2D finite element program designed to solve both 2D plane strain and axi-symmetric problems. This was used to analyse square footings of size 8, 15, and 20 cm. Additionally, equations due to Zhu et al. (2001) were used to determine the bearing capacity factors Sγ and Nγ for different footing shapes. Relaibilty of the results showed that these equations could be used for larger footings with using reduction factor for Nγ.

It was found that the bearing capacity shape factor Sγ increased slightly with increasing width of the footing, while the bearing capacity factor N_γ reduced. Model scale test results show that the bearing capacity factor, N_γ, is dependent on the absolute width of the footing for each of circular, rectangular and square footings. N_γ for dense soil decreases with increasing of footing size.

Keywords: *Scale effect, size, shape, bearing capacity, settlement, finite element analysis*

I. INTRODUCTION

Berry (1935), who studied scale effect phenomenon, presented results showed that the bearing capacity of surface model circular footings increased disproportionately with increasing footing size on a dense sand at constant relative density. Although the scale effect phenomenon seems to be fairly well recognized by many investigators, there is no provision in current design practice to take this behaviour into account.

Controversial results regarding the effect of footing size on the shape factor S_γ are obtained by Merehof (1963) who showed that S_γ calculated from his formula increases with the angle of internal friction of the soil. Mobilized friction angle of soil under foundations decreases with footing size. This reavels that the value of S_γ calculated from Meyrhof's formula decreases with footing dimensions (Zhu et al., 2001). Kusakabe et al. (1991) exhibited a similar effect of footing size on shape factor S_γ by their contrifuge experimental analytical predictions. Kusakabe et al. showed that S_γ decreases by 33% as a footing size increses from several centimeters to 3 m.

Zhu et al. (2001) studied the scale effect of strip and circular footings on bearing capacity using a numerical and experimental analysis. It was shown that the bearing capacity increses exponentially with footing dimensions. Therefore, the bearing capacity factor N_γ decreases with increasing dimension. Zhu et al. (2001) indicated that a 10-fold increase in footing dimension results in an approximetly 55% reduction of N_γ. On the other hand, the shape factor increases. It was stated that using traditional value of s_γ = 0.6 for circular and strip footings with a dimension longer than 4.5 m for a dry sand is appropriate.

Ukritchon et. al (2003) used upper and lower bound solutions for the bearing capacity factor, N_γ, for surface strip footing on a frictional soil. The analyses were to bound the exact value of N_γ, within ± 5% increasing to ± 30% as the internal friction angle increased from 5^o to 45^o.

Scale effects of shallow foundation bearing capacity on granular materials were investigated by Cerato and Lutenegger (2007) to further evaluate the trend of decreasing bearing capacity factor, N_γ, with increasing footing width, B. Model scale square and circular footing tests ranging in width from 0.025 to 0.914 m were performed on two compacted sands at three relative densities. Results of the model scale tests showed that the bearing capacity factor, N_γ, is dependent on the absolute width of the footing for both square and circular footings. Small footings were shown to have low mean stresses but high N_γ values, which indicates high operative friction angles and may be related to the curvature of the Mohr-Coulomb failure envelope.

The effect of footing width B, on bearing capacity factor, N_γ, by incorporating the variation of soil friction angle with mean principal stress studied by Kumar and Khatri (2008). They recommended that for B greater than about 0.4 m, it is possible to relate N_γ with B approximately in a linear fashion on a log-log scale.

This paper represents the experimental results considering the scale effect on bearing capacity and settlement of a footing resting on a cohesionless soil and the analyses extended by using finite element software.

Soil Properties

The selected soil is characterized using Atterberg limits, compaction test, and grain-size distribution tests. The shear strength parameters are obtained by performing direct shrear test. Table 1 shows properties of used soil which can be classified as silty gravel with sand according to Unified Soil Classification Syestem. The main reason for using this type of soil is that a wide range of characteristics and footing behaviour can be observed and compared when footings are constructed on such soils.

Table (1) Properties of the used soil.

L.L.	Gravel %	Sand %	Silt+Clay %	Max. dry unit weight (kN/m^3)	Optimum moisture content %	γ_d kN/m^3	c kN/m^2	ϕ Degree
22	60.6	25.4	14	22.5	5.5	17.4	0	37

Special Manufactured Contanier

A special container was manufactured with dimensions of (70×70) cm in cross section and (100) cm in height, is used. The frame is designed to transmit load from an upper plate to footing by a rod. A dial gauge is placed on the upper plate to record settlement of the footing. The end of the load rod can be screwed with a specific footing size and shape for a specific study. The footing is placed on the top of the soil (depth of footing D_f =0).

A set of footings is prepared for this study. The sizes of the square footings were 8×8, 10×10, 15×15, and 20×20 cm. For the rectangular footing, the dimensions 8×12, 10×15, 15×22.5, and 20×30 cm are used and for the circular footing, diameters of 8 cm, 10 cm, 15 cm, and 20 cm are used.

Bearing Capacity Equations

The bearing capacity of vertically loaded, shallow, circular foundations is almost universally calculated using the formula of Terzaghi (1943) assuming that the shear strength of soil can be represented by a linear Mohr-Coulomb failure envelope:

$$q_{ult} = 0.3 * \gamma * N_\gamma * D \quad (1)$$

in which q_{ult} is ultimate bearing capacity,

γ is unit weight of the soil,
N_γ is bearing capacity factor, and
D is footing diameter.

Other equations used to determine the bearing capacity of each footing derived from the work of Zhu et al. (2001) as shown in equations (2) and (3). It could be beneficial to note that these equations are differ from Terzhagi's and Meyrhof's bearing capacity equations because they depend on some other factors such as atmospheric pressure.

The bearing capacity (q_u) of strip footings (in kPa) by numerical method could be express as:

$$q_u = 92.1\,\mathrm{Pa}\,(\frac{\gamma\,\mathrm{B}}{\mathrm{Pa}})^{0.65} \quad (2)$$

and for circular footing:

$$q_u = 50.5\,\mathrm{Pa}(\frac{\gamma\,\mathrm{D}}{\mathrm{Pa}})^{0.69} \quad (3)$$

where Pa is atmospheric pressure (100 kPa),

B is width of the strip footing, and
D is diameter of the circular footing.

Zhu et al. (2001) produced equations for bearing capacity factors N_γ and S_γ from the characteristic analysis as:

$$N_\gamma = 184\left(\frac{\gamma.B}{Pa}\right)^{-0.35} \quad (4)$$

The shape factor of circular footings derived from the characteristic analysis given in the form of:

$$S_\gamma = 0.55\left(\frac{\gamma.B}{Pa}\right)^{0.04} \quad (5)$$

Equation (5) shows that the shape factor is not a constant; it increases slightly with footing dimension.

Labrotary Results

a. Size Effect of Circular, Rectangular, and Square Footings on Bearing Capacity and Settlement

A series of loads applied on circular footings of different diameters. Figure 1a shows the effect of shape of the

footing on settlement. It is clear from Figure 1a that the settlement of the footing increases with increasing of pressure applied on the footing.

It can also be noticed from Figure 1a that with incresing dimensions of the footing, the settlement showed the same manner of changing. Although the reasults of the settelemnt for the selected diameters are so close each to other, but the difference becomes greater for footings of larger diameters. This leads to the fact that the bearing capacity of footing increses with incresing the dimensions of the footing for such type of soil and the settlement decreases with increasing of the diameter.

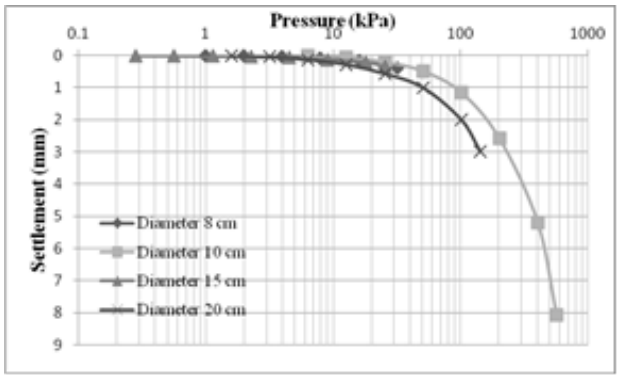

(a)

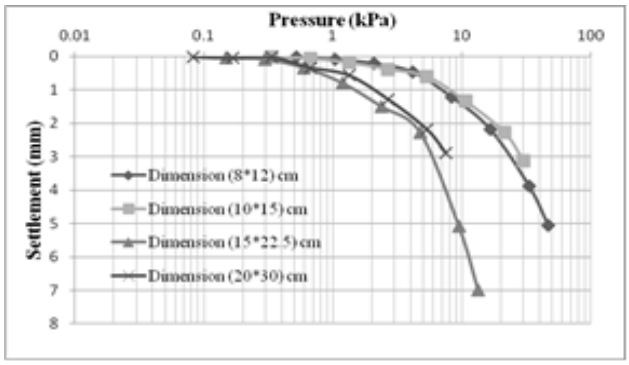

(b)

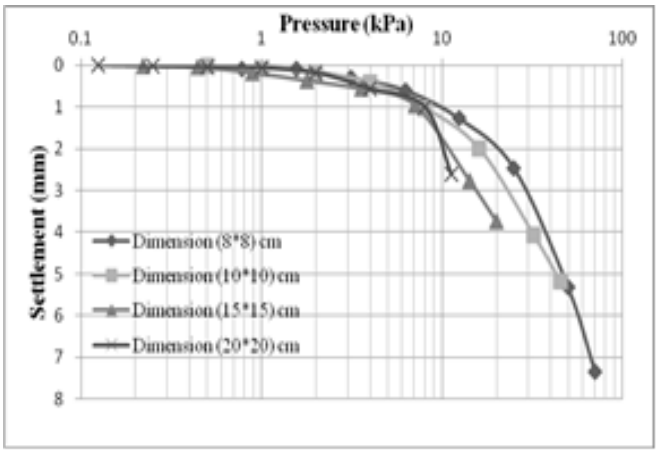

(c)

Fig. (1): Pressure-settlement relationships for: (a) circular footings, (b): rectangular footings, and (c): square footings

A series of loads is applied on the rectangular footing with different dimensions. Figure 1b shows the results of settlement for different dimensions of the footings. It is clear from the figure that the settlment increses with increasing of the pressure.It can also be noticed from Figure 1b that larger footings can sustain heavier loads. The most striking feature in the figure is that footings with dimensions 8×12 and 10×15 cm showed the same trend. In contrast, for larger footings, the sttlement was larger. This can be attributed to larger particles appered beneath the footing and rearranged under larger preesure. As mentioned before, the selected soil is granular soil with about 60% gravel. Another shape of footing which is square selected to study the effect of the shape on bearing capacity and settlement. Figure 1c shows the pressure-settlement relations obtained for square footings of different sizes. It is clear that the shape of the footing has significant effect on the footing behavior.

a. Shape Effect of Footing on Bearing Capacity and Settlement:

In this section, another effect of the footing is studied which is shape of the footing. A comparison between three groups of footings made to study effect of the shape. Firstly, circular-rectangular group, secondly, rectangular-square group, and thirdly, square-circular group. It could be said that for each group, two types of footing with different shapes are drawn together with approximately the same area to show solely effect of the shape of the footing on the bearing capacity and settlement.

1. Rectangular and Circular Shape

Figure 2a shows two different types of footing; circular and rectangular approximately with the same area. It can be noticed that the area of circular footing is 176.71 cm^2 and for rectangular footing is 150 cm^2 which they are so close to each other. It is clear from the figure that at the beginning, the settlement is approximately the same. However, at 30 kPa pressure, the circular footing cited more settlement than rectangular footing. As a result, the shape of the footing has an effect on the settlement as well as the bearing capacity. In contrast, Figure 2b seems to follow the opposite trend compared with Figure 2a.

Although the settlement of the footing is fluctuated between the two case studies in Figures 2a and b, but the bearing capacity of rectangular footing is greater than for circular. Terzaghi has established this fact for granular soil. The first term in Terzaghi's equation is always zero (see equation 1), while for the last term of the equation, Terzaghi multiply (B.Nγ) by 0.5 and 0.3 for rectangular and circular footings, respectively. This leads to the fact that for rectangular footing, the bearing capacity is almost higher than square footing. Most of the pressure-settlement curves in this study indicate local type of shear failure.

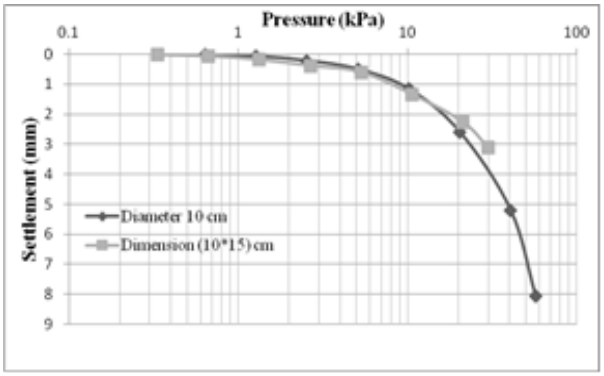

(a)

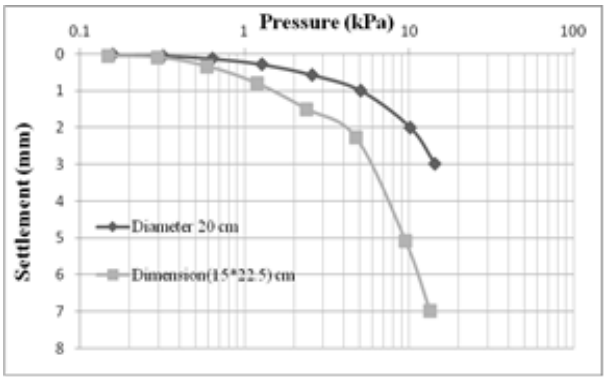

(b)

Fig. (2): Comparison between the pressure-settlement relationships: for (10*15 cm) and (D = 10 cm), (b): (15*22.5 cm) and (D = 20 cm) for rectangular and circular footings

2. Rectangular and Square Shape:

Figure 3 shows a comparison between rectangular and square footings. The difference between areas of the two footings is so small and it can be negligible. It is easy to note that for rectangular footing which has less area, the settlement is so close to square footing under the same load pressure.

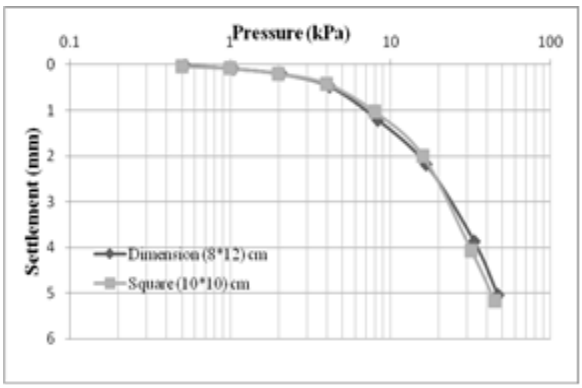

Fig. (3): Comparison between the pressure-settlement relationships for rectangular and square footings of dimensions (8*12 cm) and (10*10 cm), respectively

3. Circular and Square Shape:

Figure 4 shows another comparison which is made between square and circular footings. It could be concluded from the figure that the settlement for square footing is less than that for circular one. Not only the settlement of the square footing is lesser but also the bearing capacity of the square footing is higher than circular footing (see Figure 4). This is certainly true when Terzaghi multiplies the (B.Nγ) by 0.4 in third term of his equation for square footing, whereas, for circular footing, 0.3 used as a reduction value in the third term.

It can be noticed that equations (3), (4) and (5), which are derived by Zhu et al. (2001), are employed to obtain q_u (bearing capacity of the footing), N_γ and S_γ respectively.

It is clear from Figure 5a that S_γ increased slightly with increasing width of the footing. In contrast, the opposite scheme can be seen in Figure 5b for Nγ. The present study showed that bearing capacity factor N_γ decrease with width or diameter increasing as showing in Figure 5b.
It could be argued that the ultimate bearing capacity for strip and circular footings obtained from equations (2) and (3) increased with the width or diameter of the footing (see Figure 5c). The most striking feature in Figure 5c is that the bearing capacity for rectangular and square footings is more than the bearing capacity for circular footing of the same width or diameter. This fact also coincides with the bearing capacity equations established by Terzaghi (1943).

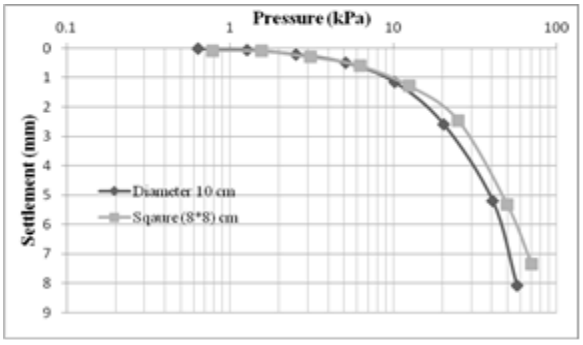

Fig. (4): Comparison between the pressure-settlement relationships for square and circular footings of dimensions (8*8 cm) and (D = 10 cm), respectively

Therefore, this will exhibit the validity of Zhu's equation to evaluate the bearing capacity for larger footings.

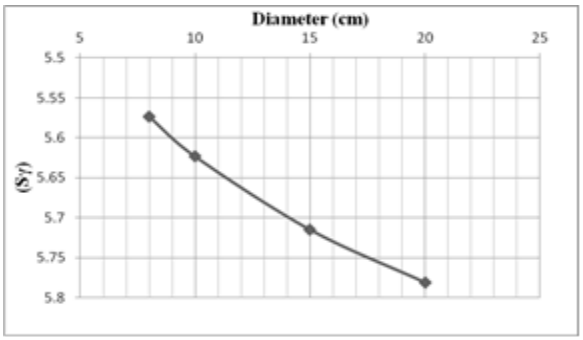

(a)

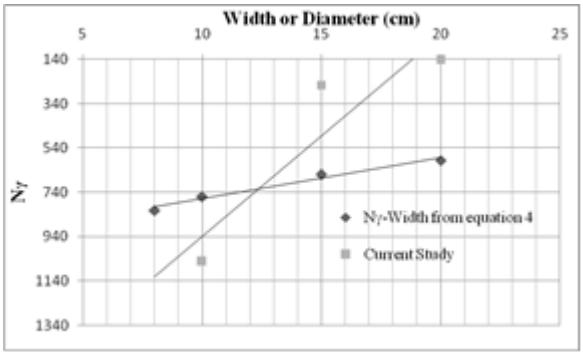

(b)

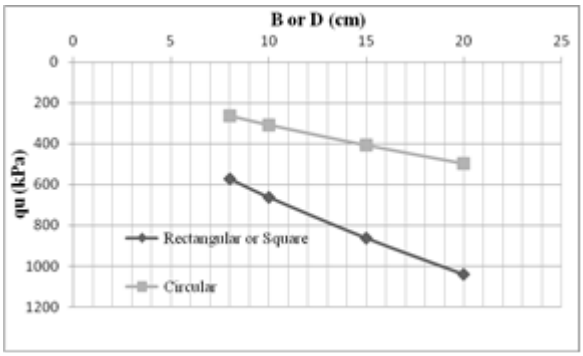

(c)

Fig. (5): Variation of: (a) Sγ,: (b) N_γ, and : (c) q_u with the dimensions of the footings

Finite Element Analysis

The analyses of finite element using New Mohr-Coulomb Elastic-Perfectly Plastic model are performed on square footing of different square footing width , namely (8, 15, 20 cm). The finite element software (SAGE-CRISP), which is a 2D finite element program designed to solve both 2D plane strain and axi-symmetric problems, is adopted. The analyses were performed along the depth of the soil geometry and along the horizontal line beneath the footing width and near the edge of the footing as shown in the finite element mesh for the plane strain problem, Figure 6. The applied load is settled at (100) kPa with drained condition, the modulus of elasticity was 3000 kPa and Poisson's ratio =0.3. Vertical displacement with increment number for nodes 1, 13, 25, 43, and 84 were drawn as shown in Figure 7.

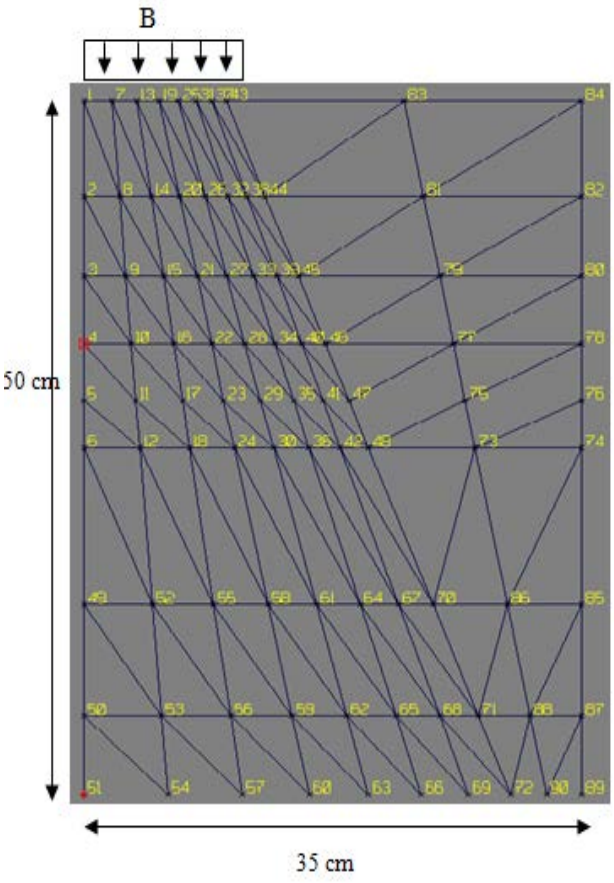

Fig. (6): Typical axi-symmetric finite element mesh used in the analysis

It can be noticed from Figure (7) that the maximum vertical displacement takes place in larger footings. Figure (8) shows the horizontal displacement for nodes 13, 25, 43, and 83.

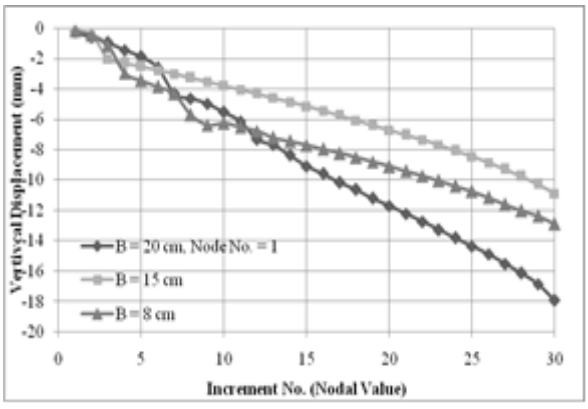

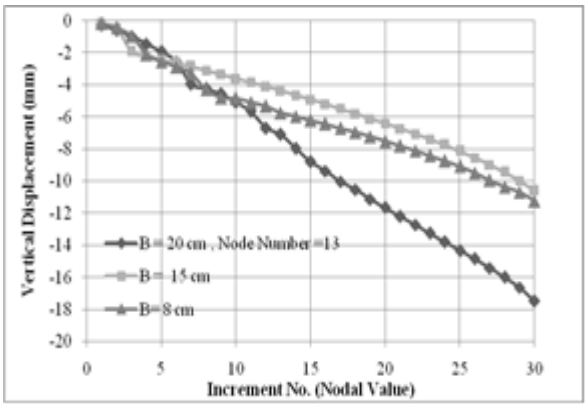

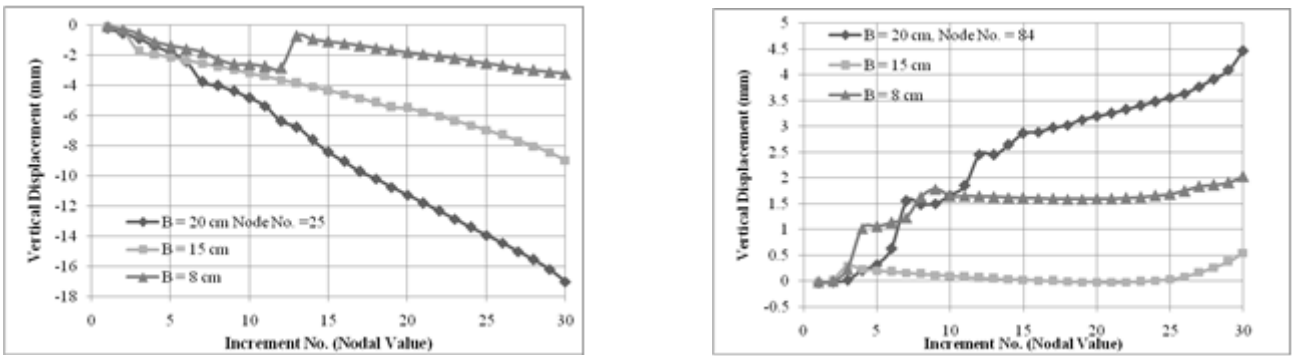

Fig. (7): Vertical displacement versus increment number for nodes 1, 13, 25 and 84

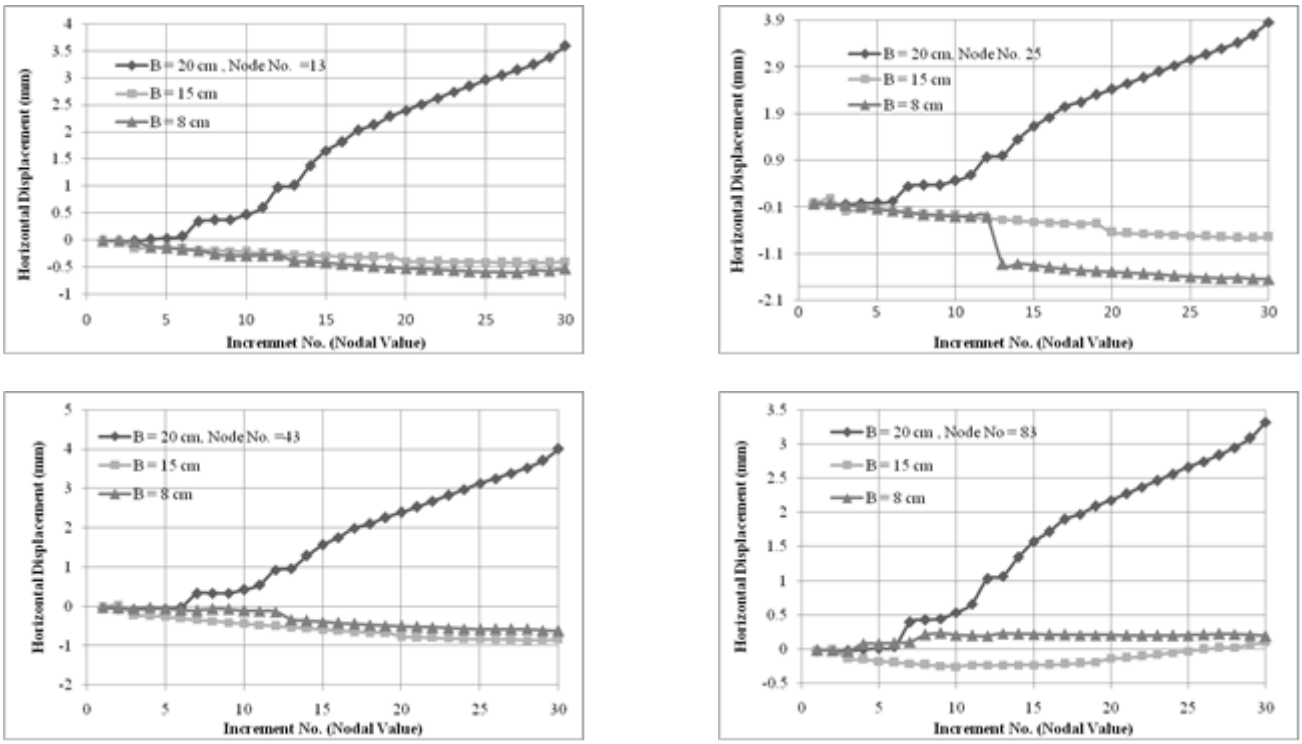

Fig. (8): Horizontal displacement versus increment number for nodes 13, 25, 43 and 83

Horizontal displacement seems to follow the same trend of vertical displacement, but the horizontal displacement is greater for larger footing width. Node 84 witnessed zero horizontal displacement. Along the depth of the mesh, the vertical displacements are drawn for different nodes, namely 1, 2, 3, 4, 5, 6, 49, and 51. Figure (9) shows the results of the vertical displacement against the increment number.

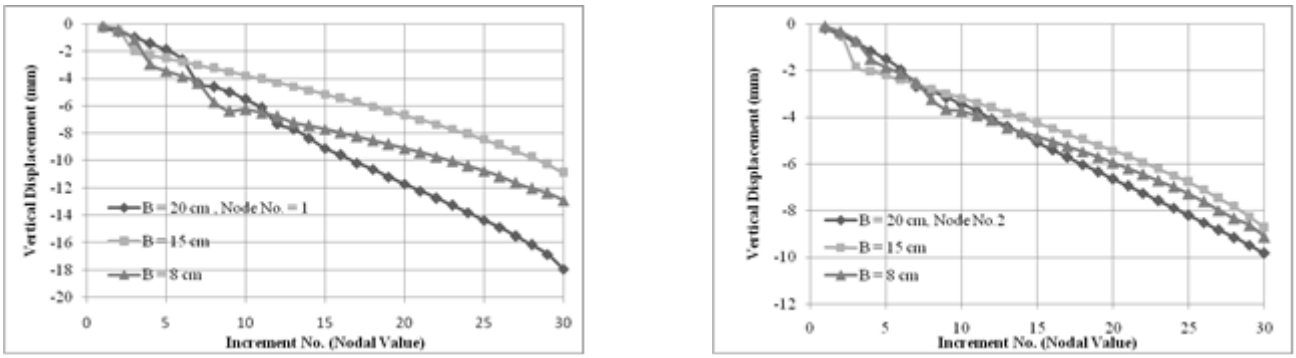

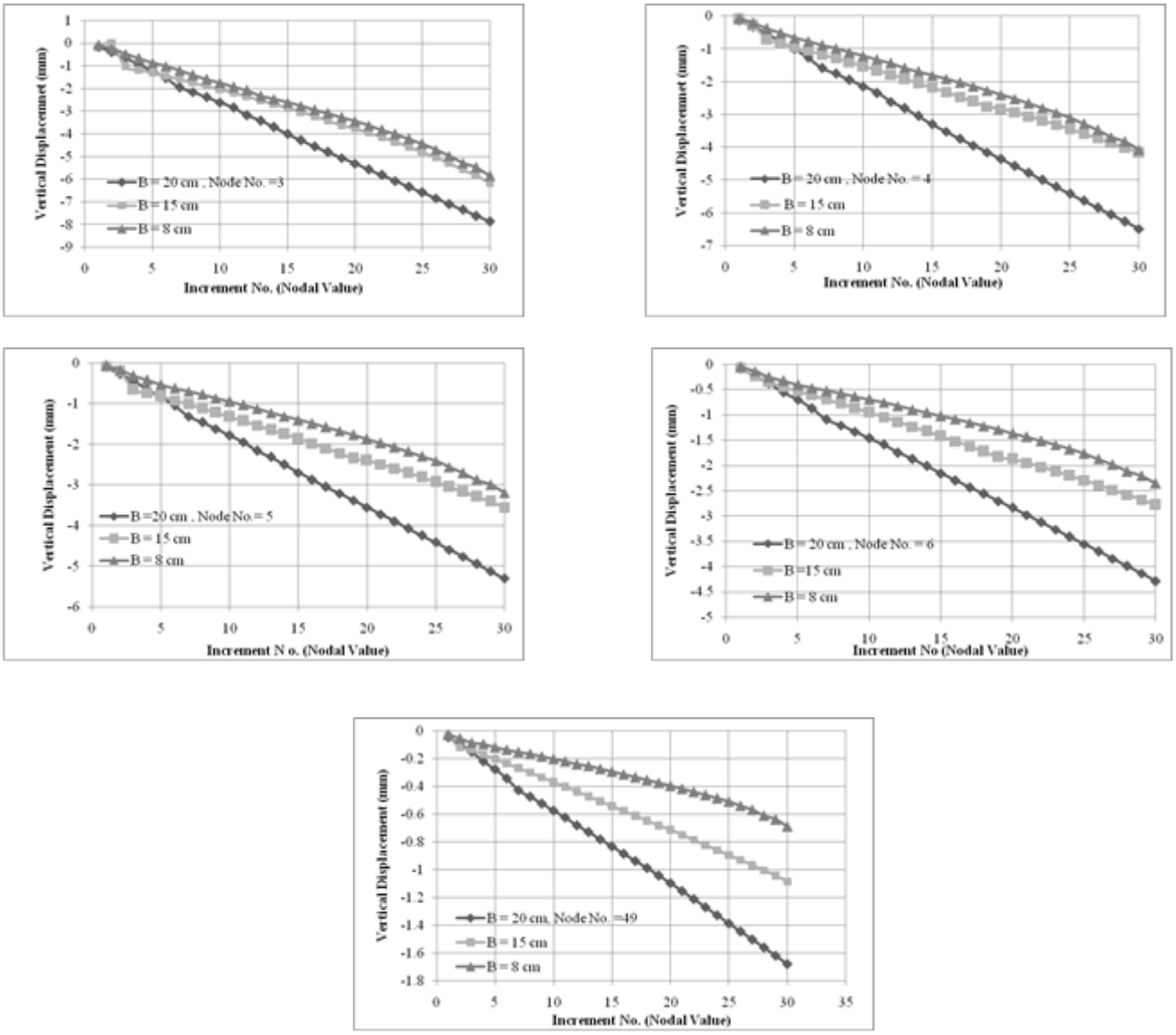

Fig. (9): Vertical displacement versus increment number for nodes 1, 2, 3, 4, 5, 6 and 49

Contour lines for the angle theta, vertical displacements and the angle of dilation were plotted. The dilation of the footing due to the loading pressure is one of the most important features for the friction soil. Therefore it can be useful to predict the most violence zone within the soil mass. Figure 10 shows angle of theta for the entire geometry of the soil.

It can be noticed from Figure 11 that the most violence zone for the angle of dilation is directly beneath the footing, where it reached approximately (-90) near node No. 84. The most striking feature in Figure (11) is that for all cases, the angle of dilation is the same. This is because small difference in the size of the footing could not affect it and it may be more pronounced for higher differences in width between the footings and for different loading cases. Figure 12 shows contour lines of vertical displacement beneath the footing. The figure reveals that increasing the footing width leads to greater settlement under the same applied load.

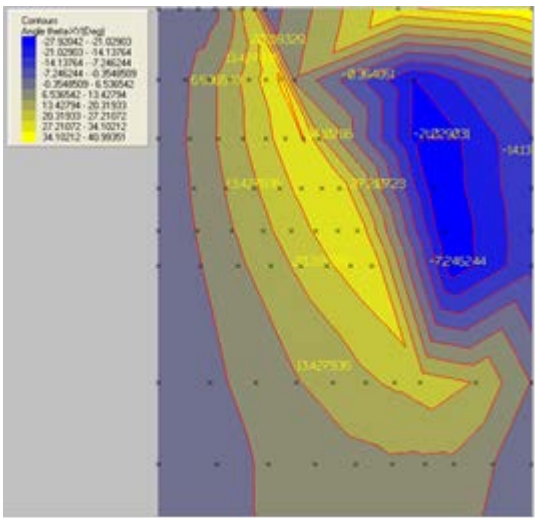

(a)

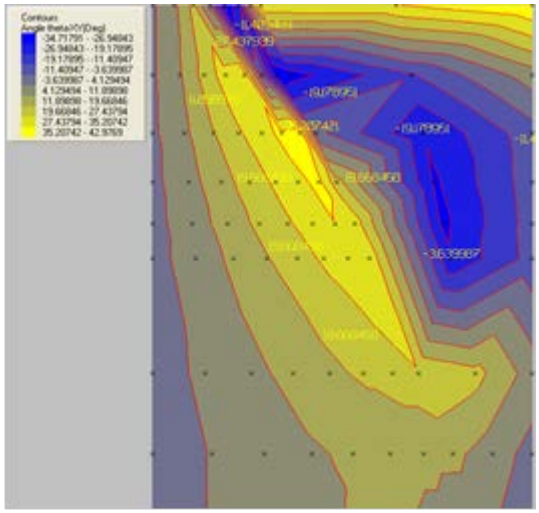

(b)

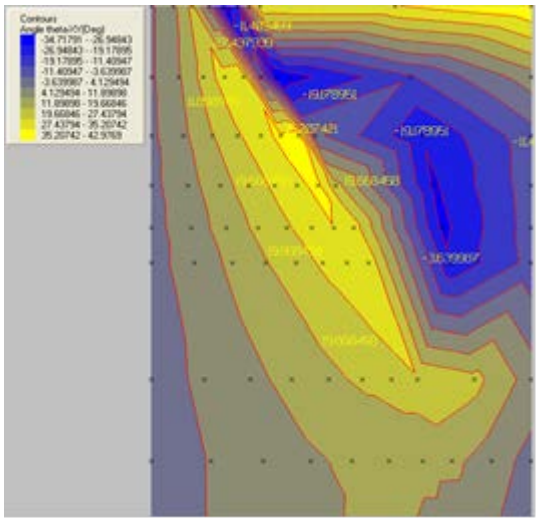

(c)

Fig. (10): Contour lines for angle of theta within the soil mass under the footings: (a) B=20 cm, (b): B= 15 cm and (c): 8 cm, load = 100 kPa

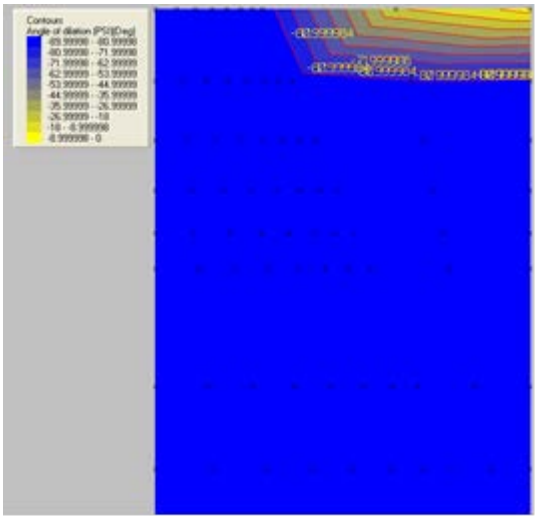

(a)

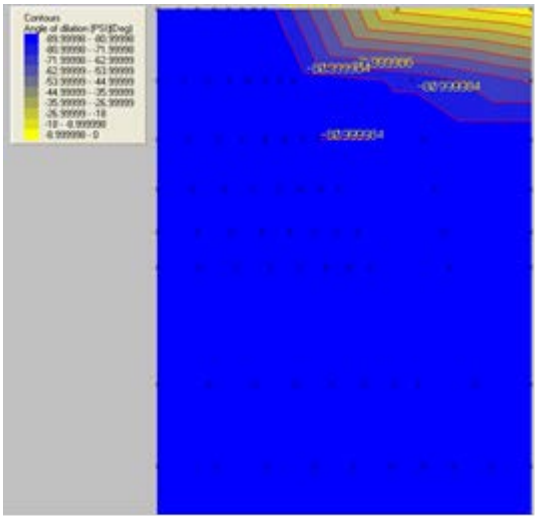

(b)

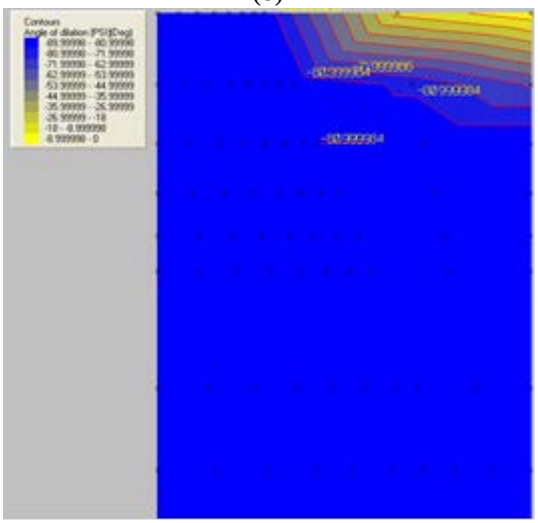

(c)

Fig. (11): Contour lines for the angle of dilation within the soil mass under the footings: (a) B=20 cm , (b): B= 15 cm and (c): 8 cm, load = 100 kPa

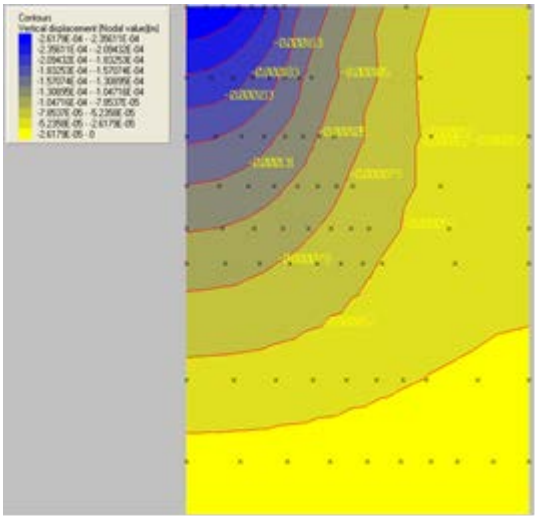

(a)

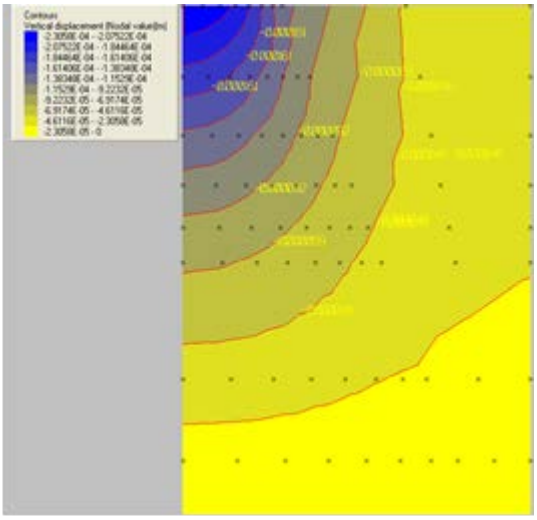

(b)

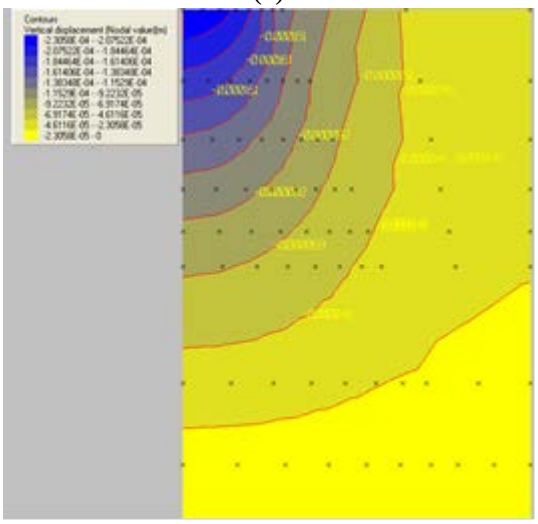

(c)

Fig. (12): Contour lines for vertical displacement within the soil mass under the footings: (a) B=20 cm, (b): B= 15 cm and (c): 8 cm, load = 100 kPa

CONCLUSIONS

1. The settlement for square footing is less than that for circular one of the same area. In addition, the bearing capacity of the square footing is greater than circular footing. This is certainly true when Terzaghi multiplies the $(B.N_\gamma)$ by 0.4 in the third term of his equation for square footing, whereas, for circular footing, 0.3 used as a reduction value for the third term.
2. The bearing capacity factor $S_\square$ increases slightly with width of the footing. In contrast, the opposite scheme for N_γ noticed.
3. Model scale test results show that the bearing capacity factor, N_γ, is dependent on the absolute width of the footing for each of circular, rectangular, and square footings. N_γ for dense soil decreases with increasing of footing size. N_γ also decreased with dimension increasing.
4. The bearing capacity for rectangular and square footings is more than the bearing capacity for circular footing of the same width or diameter. Therefore, this will exhibit the validity of Zhu's equation to evaluate the bearing capacity for larger footings.
5. Higher values of N_γ could be produced from actual model-scale footing test results than theoretical equations. Therefore, reduction factor should be used when using full scale footing design.
6. The results of finite element analyses could be used to predict the vertical displacements directly under the footing or within the soil mass. Moreover, the angle of dilation could be useful to show the most violence zone in the soil.

REFERENCES

[1] Berry, D.S. (1935), "Stability of Granular Mixtures. American Society for Testing Materials" Proceedings of the 38th Annual Meeting. Vol. 35, No. 2. pp. 491-507.

[2] Cerato, A. B. and Lutenegger, A. J., (2007), "Scale Effects of Shallow Foundation Bearing Capacity on Granular Material", Journal of Geotechnical and Geoenvironmental Engineering, ASCE, Vol. 133, No. 10, pp. 1192-1202.

[3] J.Kumar and V.N. Khatri, (2008) Effect of Footing Width on Bearing Capacity Factor, N. Journal of Geotechnical and Environmental Engineering, ASCE, Vol.134, No. 9, p.p 1299-1310.

[4] Kusakabe, O. Yamaguchi, H. and Morikage, A., (1991), "Experiment and Analysis on the Scale Effect of Nγ for Circular and Rectangular Footings", Centrifuge 1991. pp. 179-186.

[5] Manual of Limit sage Crisp (2001).

[6] Meyerhof, G.G., (1963), "Some Recent Research on the Bearing Capacity of Foundations", Canadian Geotechnical Journal. Vol. 1, No. 1. pp. 16-25.

[7] Terzaghi, K. (1943), "Theoretical Soil Mechanics", John Wiley and sons, New York.

[8] Ukritchon, B., Whittle A.J and Klangvijit, C., (2003), "Calculation of Bearing Capacity Factor N_γ Using Numerical Limit Analyses", Journal of Geotechnical and Enviromental Engineering, ASCE, Vol. 129, No.6, p.p 468-474.

[9] Zhu, F., Clark, J.I. and Phillips, R. (2001) Scale Effect of Strip and Circular Footings Resting on Dense Sand. Journal of Geotechnical and Environmental Engineering, ASCE, Vol.127, No. 7, p.p 613-621.